PCCP

PAPER

View Article Online
View Journal | View Issue

Cite this: *Phys. Chem. Chem. Phys.*, 2015, **17**, 22412

Range separated hybrids of pair coupled cluster doubles and density functionals

Alejandro J. Garza,[a] Ireneusz W. Bulik,[a] Thomas M. Henderson[ab] and Gustavo E. Scuseria*[abc]

Received 14th May 2015,
Accepted 30th July 2015

DOI: 10.1039/c5cp02773j

www.rsc.org/pccp

Pair coupled cluster doubles (pCCD) is a size-consistent, size-extensive, low-cost simplification of CCD that has been shown to be able to describe static correlation without breaking symmetry. We combine pCCD with Kohn–Sham functionals of the density and the local pair density in order to incorporate dynamic correlation in pCCD while maintaining its low cost. Double counting is eliminated by splitting the (interelectron) Coulomb operator into complementary short- and long-range parts, and evaluating the two-body energy with pCCD in the long-range and with density functionals in the short-range. This simultaneously suppresses self-interaction in the Hartree-exchange term of the functionals. Generalizations including a fraction of wavefunction two-body energy in the short-range are also derived and studied. The improvement of our pCCD+DFT hybrids over pCCD is demonstrated in calculations on benchmarks where both types of correlation are important.

1 Introduction

Many of the limitations of current Kohn–Sham density functional theory (KS-DFT) approximations are rooted in just two problems: self-interaction and static (or strong) correlation.[1] In one-electron systems, the self-interaction error (SIE) occurs when the Hartree and exchange terms do not cancel each other exactly.[2] The concept of SIE can be extended to many-electron systems,[3–5] where it manifests in deviations from linearity in the total energy when electron number is varied between consecutive integers—a constraint that the exact functional must satisfy.[6] The SIE is thus an artifact of inexact functionals. In contrast, static correlation is a physical consequence of exact or near degeneracies, particularly between frontier orbitals. Common DFT approaches fail for strongly correlated systems due to the specific approximations and paradigms that have been used to develop density functionals.[7,8]

An efficient way to reduce the SIE in KS-DFT that has been most successful in practical applications is based on the technique of range separation.[9–15] In this approach, the interelectron Coulomb operator $r_{12}^{-1} = v_{ee}(r_{12})$ is divided into complementary short-range (SR) and long-range (LR) parts

$$v_{ee}(r_{12}) = v_{ee}^{sr,\mu}(r_{12}) + v_{ee}^{lr,\mu}(r_{12}) \quad (1)$$

where, typically, $v_{ee}^{sr,\mu}(r_{12}) = r_{12}^{-1}\mathrm{erfc}(\mu r_{12})$, $v_{ee}^{lr,\mu}(r_{12}) = r_{12}^{-1}\,\mathrm{erf}(\mu r_{12})$, and μ is the range separation parameter. Range separated hybrid functionals use eqn (1) to evaluate different amounts of DFT and Hartree–Fock (HF) exchange in different ranges; inclusion of the latter reduces the SIE.[15] In particular, long-range corrected (LC) hybrids, which have large fractions of HF exchange in the LR, dramatically improve upon (semi)local functionals in the description of problems where self-interaction is pathological.[16–29]

Such a practical solution is not known for the problem of static correlation. Often, the most common path for dealing with static correlation is to abandon density functionals and work with multireference (MR) wavefunction methods, despite the latter being inefficient for capturing dynamic correlation. This limitation of traditional MR techniques, and the fact that many density functional approximations (DFAs) describe dynamic correlation in an efficient manner, has led to numerous attempts to combine MR wavefunctions with DFT.[30–62] However, MR+DFT has to deal with its own problems:

1. *The symmetry dilemma*. Typical KS-DFT approximations can break spin symmetry, particularly in strongly correlated systems. One has therefore to choose between correct spin symmetries and unphysical energies, or improved energies and unphysical spin densities. The densities provided by MR methods are symmetry-adapted and are thus inadequate for KS-DFT in these cases; although one can choose to retain the symmetry-adapted densities, this choice normally results in massive static correlation errors for common DFAs.[1] To avoid this issue, Perdew *et al.*[63] have proposed to reformulate KS-DFT in terms of the density $n(r)$ and the on-top pair density $P_2(r)$ (the probability

[a] *Department of Chemistry, Rice University, Houston, Texas, 77251-1892, USA. E-mail: guscus@rice.edu*
[b] *Department of Physics and Astronomy, Rice University, Houston, Texas, 77251-1892, USA*
[c] *Chemistry Department, Faculty of Science, King Abdulaziz University, Jeddah 21589, Saudi Arabia*

of finding two electrons at r), rather than $n(r)$ and the spin density $m_z(r)$. For a Slater determinant[64] $P_2(r) = n_\uparrow(r)n_\downarrow(r)$, and because $n(r) = n_\uparrow(r) + n_\downarrow(r)$ and $m_z(r) = n_\uparrow(r) - n_\downarrow(r)$, $m_z(r)$ in KS-DFT can be equivalently defined as

$$m(r) = \sqrt{n(r)^2 - 4P_2(r)}. \quad (2)$$

The alternative spin density $m(r)$ has proved useful to couple MR wavefunctions with KS-DFT functionals.[33,41,57,62] There are, however, a few drawbacks in this approach. When using MR densities, $m(r)$ in eqn (2) can become complex in certain strongly correlated systems.[65] Also, calculating $P_2(r)$ typically requires computation and storage of the two-particle density matrix (2PDM) Γ^{rs}_{pq}, which can be expensive.[47,48,62]

2. *Double counting*. In general, MR wavefunctions contain some dynamic correlation which is also described by DFT correlation functionals. In addition, approximate exchange functionals can mimic some static correlation effects in a nonspecific manner.[66] A way to avoid the double counting of static correlation in MR+DFT is to add only DFA correlation (which is assumed to be purely dynamical) to the MR energy; the double counting of dynamic correlation can then be approximately eliminated *via* a local scaling factor of the correlation energy density,[41–43] or other conceptually similar partition schemes.[44,45] Alternatively, one can divide the $v_{ee}(r)$ operator into complementary parts to create global[53,57,62] (*i.e.*, having a constant fraction of wavefunction two-body energy through the full-range) or range-separated[38,54,58,61] MR+DFT hybrids that eliminate double counting exactly, at the cost of including DFT exchange (which can introduce self-interaction). Considering the above discussion regarding LC-DFT, analogous LC-MR+DFT hybrids seem particularly appealing. We note that, although some of the first LC-MR+DFT implementations offered rather unsatisfactory results for strongly correlated systems[38] (*e.g.*, very large μ values and active spaces were needed to obtain good energies), these combinations did not addres the symmetry dilemma. As another option, some new approaches,[59,60] based on embedding theories,[67,68] propose to separate the correlations in orbital space, rather than real space (as is done in the hybrids).

3. *Problems of the MR method*. Traditional MR methods of quantum chemistry have poor scaling and suffer from size-consistency and size-extensivity issues. These problems are inherited in MR+DFT and the only solution is to substitute the commonly used MR wavefunctions by novel methods for static correlation. The use of mean-field projected Hartree–Fock[69] (PHF) methods combined with DFT has been suggested for overcoming the problem of poor scaling with system size.[55,56] However, PHF still lacks size-consistency and size-extensivity.[69] Recently, the density matrix renormalization group[70] (DMRG) algorithm has also been proposed as an alternative.[61] Also recently,[62] we have proposed global hybrids of pair coupled cluster doubles[71–76] (pCCD) and DFT, which are motivated by various features of pCCD that make it particularly suitable for MR+DFT.

In this paper, we propose the use of LC hybrids of pCCD and DFT as MR+DFT methods that elude the above problems without introducing further undesirable features. In short, LC-pCCD+DFT comes as a rather logical consequence of the discussion here so far: the 2PDM, Γ^{rs}_{pq}, of pCCD has a simple structure with only $2N^2$ nonzero elements in the natural orbital basis,[76] allowing the use of the $P(r)$ formulation of KS-DFT to avoid the symmetry dilemma with negligible increase in computational cost; the range separation with long-range correction eliminates double counting, and simultaneously suppresses the SIE; pCCD is size-extensive, size-consistent, and has low scaling[76] (formally $\mathcal{O}(N^3)$, neglecting the basis transformation of the two-body interaction). One possible drawback though is that pCCD requires an orbital optimization to define the pairing scheme (see below). This is nontrivial and can suffer from multiple solutions, which may affect the DFT energies. However, in practice we have not found problems with this potential issue so far. We also derive generalizations of LC-pCCD+DFT that include a fraction of pCCD two-body energy in the short range, and test these hybrids on benchmarks where both types of correlation are important. Our work here is thus and extension and generalization of our previous efforts on pCCD+DFT.[62]

2 Theory and methods

2.1 pCCD

Let i and a be indices for occupied and virtual orbitals, respectively. The pCCD ansatz is[71–76]

$$|\Psi\rangle = e^{\hat{T}}|0\rangle, \quad (3)$$

where $|0\rangle$ is an optimized, closed-shell, reference determinant and

$$\hat{T} = \sum_{ia} t_i^a c_{a\uparrow}^\dagger c_{a\downarrow}^\dagger c_{i\downarrow} c_{i\uparrow}. \quad (4)$$

Thus, pCCD is a simplification of the well-known CCD method that restricts excitations to pair excitations (plus orbital optimization). Despite this, pCCD has been shown to describe static correlation without symmetry breaking.[71–76] In fact, it is exact for two-electron systems and its wavefunction closely reproduces that of a seniority-zero full configuration interaction—an optimal linear combination of all configurations that do not break electron pairs[76] (*i.e.*, all seniority zero configurations; see ref. 77 for a detailed explanation of the concept of seniority). As we have noted before,[62] pCCD is especially suitable for MR+DFT: pCCD is (always) size-extensive and size-consistent (provided that $|0\rangle$ be size-consistent); the equations for the t_i^a amplitudes can be solved in $\mathcal{O}(N^3)$ time and the orbital optimization can be done efficiently; Γ^{rs}_{pq} has a simple structure with only $2N^2$ nonzero elements in the natural orbital basis.[76] For a detailed description of pCCD and the formulas for Γ^{rs}_{pq}, see ref. 76.

One last technical detail regarding pCCD should be mentioned here. Like other coupled cluster methods, pCCD has a right-hand eigenvector $e^{\hat{T}}|0\rangle$ and left-hand eigenvector $\langle 0|(1 + \hat{Z})e^{-\hat{T}}$, where $\hat{Z}$ is defined analogously to $\hat{T}\dagger$ in eqn (4) (*i.e.*, the t_i^a amplitudes are replaced by the z_i^a amplitudes of the left-hand eigenvector). In practice, we evaluate operators by weighting the elements of the one- and two-particle density matrices of pCCD with their corresponding one- and two-electron integrals, respectively. This is equivalent to saying that we evaluate the expectation

value of an operator $\hat{O}$ as $\langle 0|(1+\hat{Z})e^{-\hat{T}}\hat{O}e^{\hat{T}}|0\rangle$. In what follows, we shall denote $\langle 0|(1+\hat{Z})e^{-\hat{T}}\hat{O}e^{\hat{T}}|0\rangle$ as $\langle\Psi|\hat{O}|\Psi\rangle$ whenever $|\Psi\rangle$ is the pCCD $e^{\hat{T}}|0\rangle$ wavefunction.

2.2 Alternative densities

As in previous works (see, *e.g.*, ref. 33, 41, 57, 62), we use the $P_2(r)$ formulation (eqn (2)) of KS-DFT[63] to circumvent the symmetry dilemma. The alternative spin density is defined as

$$m(r) = \begin{cases} \sqrt{n(r)^2 - 4P_2(r)} & \text{if } n(r)^2 \geq 4P_2(r) \\ 0 & \text{if } n(r)^2 < 4P_2(r) \end{cases}, \quad (5)$$

to prevent $m(r)$ in eqn (2) from becoming complex. For generalized gradient approximations (GGAs), we adopt the translated gradient spin density of ref. 57

$$m'(r) = \begin{cases} n'(r)\sqrt{1 - \dfrac{4P_2(r)}{n(r)^2}} & \text{if } n(r)^2 \geq 4P_2(r) \\ 0 & \text{if } n(r)^2 < 4P_2(r) \end{cases}, \quad (6)$$

where $n'(r) = |\nabla n(r)|$. Eqn (6) has already been shown to produce reasonable results.[57,62]

In the introduction section, we mentioned that one may choose to retain the symmetry-adapted $[n,m_z]$ densities of the MR wavefunction. For comparison purposes, we will show calculations using both the $[n,m_z]$ densities and the alternative $[n,m]$ densities. We note that all benchmarks studied here are singlets and therefore $[n,m_z] = [n,0]$ (*i.e.*, because pCCD preserves spin symmetry).

2.3 LC-pCCD-DFT

In this approach the electronic energy is evaluated as

$$E = \langle\Psi|\hat{\mathscr{H}}_{\text{core}} + \hat{v}_{\text{ee}}^{\text{lr},\mu}|\Psi\rangle + E_{\text{Hx}}^{\text{sr},\mu}[n,m] + E_{\text{c}}^{\text{sr},\mu}[n,m], \quad (7)$$

where $|\Psi\rangle$ is the pCCD wavefunction, $\hat{\mathscr{H}}_{\text{core}}$ the one-electron core Hamiltonian, $\hat{v}_{\text{ee}}^{\text{lr},\mu} = \sum_{i\leq j} r_{ij}^{-1} erf(\mu r_{ij})$, $E_{\text{Hx}}^{\text{sr},\mu}$ is the SR DFT Hartree-exchange term, and $E_{\text{c}}^{\text{sr},\mu}$ the SR DFT correlation. In this work, we calculate $|\Psi\rangle$ with the full Hamiltonian self-consistently using in-house programs; the evaluation of eqn (7) is then carried out in a modified version of *Gaussian*.[78] Thus, we assume that the effect of self-consistency is small when replacing the SR pCCD two-body energy with the corresponding DFT terms. This assumption is reasonable because it has been shown that, in MR+DFT, the error due to the approximate functional is often larger than the error due to the lack of self-consistency.[79] We also remark that the non-self-consistent application of eqn (7) is analogous to the LC-MR+DFT method of Pollet *et al.*,[38] except that here we use the alternative $[n,m]$ densities and a pCCD wavefunction, rather than symmetry-adapted $[n,m_z]$ densities and a configuration interaction (CI) wavefunction.

To evaluate $E_{\text{Hx}}^{\text{sr},\mu}$ and $E_{\text{c}}^{\text{sr},\mu}$, we employ the range-separated parametrization of the local density approximation (LDA) by Paziani *et al.*[80] For combinations with GGAs, we use, for the exchange, the long-range correction by Iikura *et al.*[10] (LC-PBE) that is implemented in *Gaussian*, and we also compare with results using LC-ωPBE exchange.[13] Although there are some LC-GGA parametrizations for the correlation,[81,82] for simplicity (and possible extension to meta-GGAs) we introduce an approximate local scaling

$$E_{\text{c}}^{\text{sr},\mu}[n,m] = \int n(r)\frac{\varepsilon_{\text{c},\mu}^{\text{sr}-\text{LDA}}(n,m)}{\varepsilon_{\text{c}}^{\text{LDA}}(n,m)}\varepsilon_{\text{c}}^{\text{GGA}}(n,m,n',m')\text{d}^3r \quad (8)$$

where $\varepsilon_{\text{c},\mu}^{\text{sr}-\text{DFA}}$ and $\varepsilon_{\text{c}}^{\text{DFA}}$ are short- and full-range correlation energy densities, respectively. As will be shown later, this simple correction works considerably well. We note, in passing, that eqn (8) can also be used to combine GGAs (or meta-GGAs) with other types of correlated methods as in, *e.g.*, the LC-ωDFT + dRPA method of Janesko *et al.*[83] which incorporates LR correlation from the direct random phase approximation (dRPA) in order to describe van der Waals interactions.

2.4 LC-pCCD-λDFT

LC-pCCD-DFT can be generalized to include a fraction of wavefunction two-body energy in the short range (analogous to, *e.g.*, the Coulomb-attenuating method[11] in standard KS-DFT). To do this, we follow closely the procedure used by Sharkas *et al.*[53] to derive MR+DFT global hybrids. Let us split $\hat{v}_{\text{ee}}^{\text{sr},\mu} = \sum_{i\leq j} r_{ij}^{-1} erfc(\mu r_{ij})$ as

$$\hat{v}_{\text{ee}}^{\text{sr},\mu} = \lambda\hat{v}_{\text{ee}}^{\text{sr},\mu} + (1-\lambda)\hat{v}_{\text{ee}}^{\text{sr},\mu}, \quad (9)$$

where $\lambda \in [0,1]$. If λ is the fraction of SR wavefunction two-body energy included, then we can write the electronic energy as

$$E = \langle\Psi|\hat{\mathscr{H}}_{\text{core}} + \hat{v}_{\text{ee}}^{\text{lr},\mu} + \lambda\hat{v}_{\text{ee}}^{\text{sr},\mu}|\Psi\rangle + \bar{E}_{\text{Hxc}}^{\text{sr},\mu,\lambda}[n], \quad (10)$$

where $\bar{E}_{\text{Hxc}}^{\text{sr},\mu,\lambda}[n]$ is the λ-dependent Hartree-exchange–correlation term associated with the $(1-\lambda)\hat{v}_{\text{ee}}^{\text{sr},\mu}$ interaction. Because $E_{\text{Hx}}^{\text{sr},\mu}$ is linear on the $\hat{v}_{\text{ee}}^{\text{sr},\mu}$ interaction, the Hartree-exchange contribution is

$$\bar{E}_{\text{Hx}}^{\text{sr},\mu,\lambda}[n] = (1-\lambda)E_{\text{Hx}}^{\text{sr},\mu}[n]. \quad (11)$$

The KS-DFT correlation contains corrections to the kinetic energy and is not linear in λ. However, the correlation correction corresponding to $(1-\lambda)\hat{v}_{\text{ee}}^{\text{sr},\mu}$ can still be written as $\bar{E}_{\text{c}}^{\text{sr},\mu,\lambda}[n] = E_{\text{c}}^{\text{sr},\mu}[n] - E_{\text{c}}^{\text{sr},\mu,\lambda}[n]$, where $E_{\text{c}}^{\text{sr},\mu,\lambda}[n]$ is the correlation with a $\lambda\hat{v}_{\text{ee}}^{\text{sr},\mu}$ interaction. Using the scaling relation[84]

$$E_{\text{c}}^{\text{sr},\mu,\lambda}[n] = \lambda^2 E_{\text{c}}^{\text{sr},\mu/\lambda}[n_{1/\lambda}] \quad (12)$$

where $n_{1/\lambda}(r) = (1/\lambda)^3 n(r/\lambda)$, and neglecting the scaling of the density as in ref. 53, we obtain

$$\bar{E}_{\text{c}}^{\text{sr},\mu,\lambda}[n] = E_{\text{c}}^{\text{sr},\mu}[n] - \lambda^2 E_{\text{c}}^{\text{sr},\mu/\lambda}[n]. \quad (13)$$

We can then get a practical generalization of eqn (7) that includes pCCD SR two-body energy as

$$\begin{aligned} E &= \langle\Psi|\hat{\mathscr{H}}_{\text{core}} + \hat{v}_{\text{ee}}^{\text{lr},\mu} + \lambda\hat{v}_{\text{ee}}^{\text{sr},\mu}|\Psi\rangle + (1-\lambda)E_{\text{Hx}}^{\text{sr},\mu}[n,m] \\ &\quad + E_{\text{c}}^{\text{sr},\mu}[n,m] - \lambda^2 E_{\text{c}}^{\text{sr},\mu/\lambda}[n,m]. \end{aligned} \quad (14)$$

Eqn (14) suppresses the double counting in the SR exactly modulo uniform scaling effects. However, the impact of density scaling has been shown to be small for MR+DFT global hybrids[53] (less than 1 kcal mol^{-1} on average errors in thermochemistry).

Table 1 Summary of pCCD+DFT hybrid methods. The density n and alternative spin density m are calculated from the self-consistent pCCD wavefunction $|\Psi\rangle$

Method	Electronic energy formula
pCCD+1DFT	$\langle\Psi\|\hat{\mathscr{H}}_{\text{core}}+\hat{v}_{\text{ee}}\|\Psi\rangle+E_{\text{c}}[n,m]$
pCCD-DFT[a]	$\langle\Psi\|\hat{\mathscr{H}}_{\text{core}}\|\Psi\rangle+E_{\text{Hx}}[n,m]+E_{\text{c}}[n,m]$
pCCD-λDFT	$\langle\Psi\|\hat{\mathscr{H}}_{\text{core}}+\lambda\hat{v}_{\text{ee}}\|\Psi\rangle+(1-\lambda)E_{\text{Hx}}[n,m]+(1-\lambda^2)E_{\text{c}}[n,m]$
LC-pCCD-DFT	$\langle\Psi\|\hat{\mathscr{H}}_{\text{core}}+\hat{v}_{\text{ee}}^{\text{lr},\mu}\|\Psi\rangle+E_{\text{Hx}}^{\text{sr},\mu}[n,m]+E_{\text{c}}^{\text{sr},\mu}[n,m]$
LC-pCCD-λDFT	$\langle\Psi\|\hat{\mathscr{H}}_{\text{core}}+\hat{v}_{\text{ee}}^{\text{lr},\mu}+\lambda\hat{v}_{\text{ee}}^{\text{sr},\mu}\|\Psi\rangle+(1-\lambda)E_{\text{Hx}}^{\text{sr},\mu}[n,m]+E_{\text{c}}^{\text{sr},\mu}[n,m]-\lambda^2E_{\text{c}}^{\text{sr},\mu/\lambda}[n,m]$

[a] Denoted as pCCD-0DFT in ref. 62.

Also, although approximate scaling relations such as $E_{\text{c}}[n_{1/\lambda}]=\lambda E_{\text{c}}[n]$ have been used to develop functionals,[85] we observed that, in our case, using this relation affords essentially the same results as neglecting the scaling with a slightly different λ value.

For convenience, we summarize all the methods for which we present results in Table 1. Note that, at $\lambda=0$, eqn (7) and (14) are equivalent. Likewise, at $\mu=0$, eqn (14) is equivalent to our previous pCCD-λDFT method. For $\lambda=0$ and $\mu=0$, pCCD-DFT is analogous to the multiconfiguration pair density functional theory of Li Manni *et al.*,[57] except that the former uses a pCCD wavefunction while the latter uses a complete active space (CAS) wavefunction. We also remark that, with $\lambda\neq0$ and $\mu\neq0$, the LC-pCCD-λDFT energy formula bears close resemblance with that of the double hybrid DFT using the Coulomb-attenuating method[11] of Cornaton and Fromager.[58]

The pCCD+DFT combinations in Table 1 have up to two parameters: λ and μ. In this work we utilize $\lambda=3/4$ and $\mu=0.4$ bohr^{-1} due to the following reasons: (1) these values provide reasonable results for all benchmarks tested here, (2) $\lambda=3/4$ was employed for pCCD-λDFT in ref. 62, where it was also shown to be an adequate choice, and (3) $\mu=0.4$ au is commonly employed in standard KS-DFT range separated hybrids, and has been shown to be adequate for LC-MR+DFT.[86] We note, however, that the optimal μ value in common LC-KS-DFT approximations depends on the size of the system,[87] and that definition of a locally-dependent $\mu(r)$ is also possible.[88,89] However, a size-dependent μ breaks size consistency and extensivity,[29,90] whereas implementation and efficiency issues arise in the case of a locally-dependent $\mu(r)$.[89]

3 Results and discussion

3.1 Analysis of H_2 system and SR-DFT energy

Although pCCD is exact for two-electron systems, analyzing the dissociation of the H_2 molecule (Fig. 1) provides great insight on the properties of LC-pCCD+DFT methods. Only results by LDA-based hybrids are shown in Fig. 1; calculations using the Perdew–Burke–Ernzerhof[91] (PBE) functional yield very similar curves. Because of the exactness of pCCD and the nonzero $E_{\text{c}}^{\text{DFT}}[n]$, adding raw full-range DFT correlation to the pCCD energy (pCCD+1DFT) results in double counting and, consequently, too low total energies and a too high dissociation energy. The hybrids, LC-pCCD-DFT and pCCD-λDFT, suppress this double counting *via* the splitting of $\hat{v}_{\text{ee}}$. When using the alternative densities

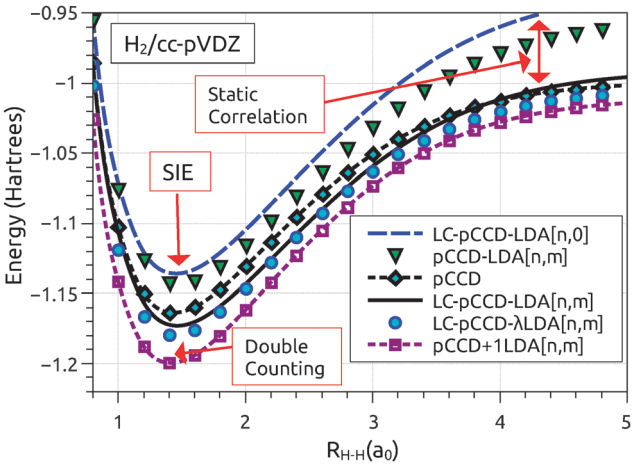

Fig. 1 Dissociation energy profiles for the hydrogen molecule. The pCCD curve is equal to FCI for this system. Hybrid methods use $\lambda=3/4$ and $\mu=0.4$ au. The input densities for the functional are indicated in brackets.

$[n,m]$, they are slightly below pCCD, but this can be attributed mostly to basis set (incompleteness) effects. This is so because the SR dynamic correlation, which is the part of the correlation most dependent on basis set size, is described (totally or in part) by the LDA, which has small basis set dependence. Note that the inclusion of pCCD two-body energy (*via* the range separation) and the use of the alternative spin density m are both important to achieve good results. This is demonstrated by the poor performance of LC-pCCD-LDA$[n,0]$ and pCCD-LDA$[n,m]$; the energies of these methods are too high because of a combination of self-interaction and static correlation errors (see below).

To analyze the sources of error for the hybrid methods in Fig. 1, we note that all of the error in the case of H_2 comes from the DFA. This error can be divided into two parts: (1) the error in the exchange, which for singlet H_2 is simply $E_{\text{x}}+0.5E_{\text{H}}$, and (2) the error in the correlation, which is the total error minus the error in the exchange. These errors are plotted for various methods in Fig. 2. For both LC-pCCD-LDA$[n,0]$ and pCCD-LDA$[n,m]$ the total error at short bond lengths and near the equilibrium is dominated by a positive contribution from the error in E_{x}, which can be interpreted as SIE. In contrast, at large internuclear distances, the largest contribution to the error comes from the E_{c}, because the LDA correlation functional cannot describe static correlation properly. The effect of the long-range correction is to reduce

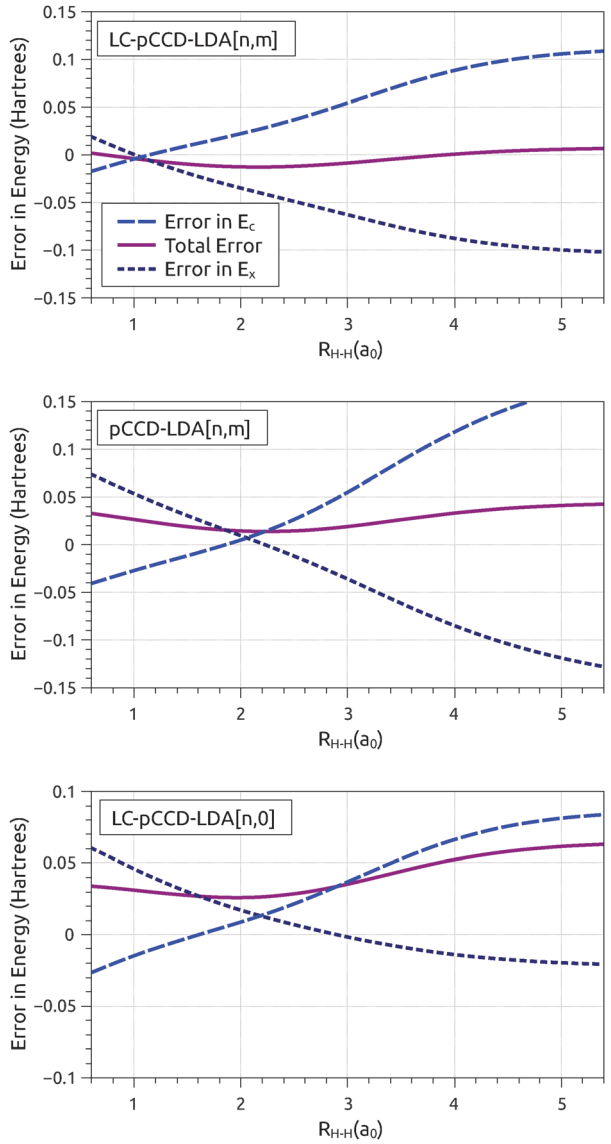

Fig. 2 Errors in the exchange and correlation for various methods in the dissociation the hydrogen molecule. Hybrid methods use λ = 3/4 and μ = 0.4 au.

the SIE, whereas the use of the alternative spin polarization results in a better cancellation of error between the exchange and correlation. Thus, LC-pCCD-LDA[n,m] provides small errors along all the dissociation curve even if the individual errors in E_x or E_c are large at the dissociation limit. In other words, the use of the [n,m] densities allows for the exchange functional to describe the static correlation missing in E_c. This explains the rather disappointing results for strongly correlated systems of previous, similar, LC-MR+DFT methods that did not employed alternative densities.[38] For example, the LC-CI-DFT[n,0] method of ref. 38 with μ = 0.45 au cannot recover more than about 75% of the correlation (with respect to restricted HF) for H_2 at R_{H-H} = 3.0 au. In fact, for this same case, even if one chooses an optimal μ value to be as close as possible to full configuration interaction (FCI), LC-CI-DFT[n,0] is not better than CI alone; the optimal μ values are extremely large[38] ($\mu \geq 5.75$ au).

The improved description of the H_2 dissociation limit by LC-pCCD-DFT when using the [n,m] densities, rather than [n,0], can be demonstrated analytically for the limit of large μ using results from ref. 92. There, an asymptotic expansion for the SR Hartree term in the $\mu \to \infty$ limit was found to be

$$E_H^{sr,\mu} = \frac{\sqrt{\pi}A_0}{\mu^2}\int n(r)^2 dr - \frac{\sqrt{\pi}A_2}{12\mu^4}\int |\nabla n(r)|^2 dr + \cdots, \quad (15)$$

where $A_k = \Gamma((k+3)/2)$. The analogous expression for the LDA exchange is[92,93]

$$E_x^{sr,\mu} = -\frac{\sqrt{\pi}A_0}{2\mu^2}\int n(r)^2 dr + \frac{3^{\frac{2}{3}}\pi^{\frac{11}{16}}A_2}{20\mu^4}\int n(r)^{\frac{8}{3}} dr + \cdots \quad (16)$$

In terms of the $n_\uparrow$ and $n_\downarrow$ densities, the LDA exchange for a spin polarized system is

$$E_x[n_\uparrow, n_\downarrow] = \frac{1}{2}\left(E_x[2n_\uparrow] + E_x[2n_\downarrow]\right). \quad (17)$$

At the dissociation limit, $P_2(r) = 0$ and thus the alternative spin polarization is $m = n$. When using the alternative densities, $2n_\uparrow = n + m = 2n$ and $2n_\downarrow = n - m = 0$, so it is readily seen that the dominant (first) terms of the Hartree (eqn (15)) and exchange (eqn (16) and (17)) energies will cancel each other. In contrast, if no alternative spin polarization is used, $m = 0$ and hence $n_\uparrow = n_\downarrow = n/2$, so that the exchange is simply $E_x^{sr,\mu}[n]$ and the difference is roughly equal to $0.5E_H^{sr,\mu}[n]$. This results in too high energies for the -LDA[n,0] approach because the LR two-body pCCD energy is already exact and equal to the full-range two-electron repulsion of $1/R_{H-H}$. Although this error could, in principle, be corrected by the correlation functional, in practice it does not because the LDA correlation is too small to account for the relatively large effects of static correlation.

Another two results from ref. 92 that are worth mentioning here are the closed-shell exact SR expansions in the limit of large μ for the exchange[92,93]

$$E_{x,exact}^{sr,\mu} = -\frac{\sqrt{\pi}A_0}{2\mu^2}\int n(r)^2 dr + \frac{\sqrt{\pi}A_2}{24\mu^4}\int n(r) \times \left(\frac{|\nabla n(r)|^2}{2n(r)} + 4\tau(r)\right) dr + \cdots \quad (18)$$

and correlation[92]

$$E_{c,exact}^{sr,\mu} = \frac{2\sqrt{\pi}A_0}{\mu^2}\int \left(P_2(r) - n(r)^2/4\right) dr + \frac{4\sqrt{\pi}A_1}{3\mu^3}\int P_2(r) dr + \cdots, \quad (19)$$

where $\tau(r)$ is the kinetic energy density. The importance of these results is that they show that, for large μ, the exact SR exchange–correlation energy is a (semi)local functional of the density and the on-top pair density, which further motivates LC-MR+DFT hybrids employing the $P_2(r)$ formulation of KS-DFT. We note that the above formulas can be used as a functional for LC-pCCD+DFT, but are not very practical because large values of μ ($\sim$2 au or greater) are required, and this leads to little change in the energy with respect to pure pCCD.

3.2 Other benchmarks

The dissociation energy profiles for linear H_4 and H_6 chains and water (HOH angle = 104.474°) are plotted in Fig. 3. Only results for hybrid methods using the [n,m] densities and incorporating a fraction of pCCD two-body energy are shown because, as discussed above, these two factors are important for describing static correlation and suppressing the SIE, respectively; the problems of LC-pCCD-DFT[n,0] and pCCD-DFT[n,m] observed in Fig. 1 for H_2 extend to other systems. The panels on the left of Fig. 3 display data for LDA-based hybrids, while those on the right do so for PBE-based methods. Dissociation curves from unrestricted coupled cluster singles and doubles with perturbative triples[94] [UCCSD(T)] are also provided as reference. The best agreement with UCCSD(T) and available experimental data is given by the LC-pCCD-λLDA and -λPBE methods, whereas hybrids that do not include SR pCCD two-body energy tend to overbind (although results are still much better than the raw addition of E_c^{DFT} to pCCD in the +1DFT methods). Comparison of LC-pCCD-λDFT data

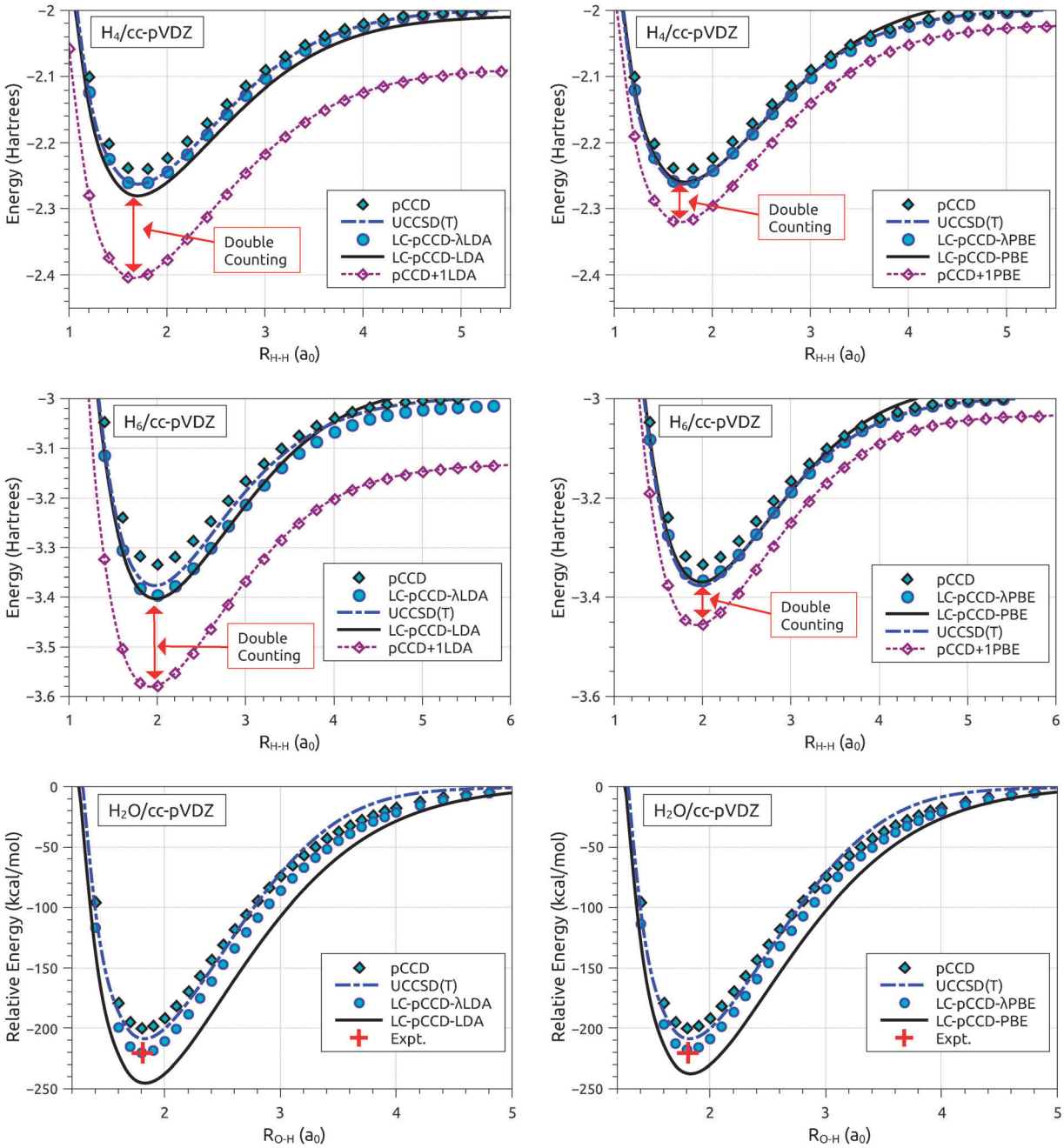

Fig. 3 Dissociation energy profiles for linear hydrogen chains and H_2O [HOH angle = 104.474°]. Hybrid methods use λ = 3/4 and μ = 0.4 au. All pCCD+DFT combinations use the [n,m] densities. Relative energies are with respect to the molecule at the dissociation limit. Cartesian basis sets are employed in all calculations.

with pCCD and pCCD+1DFT indicates that the former is effective at adding dynamic correlation to pCCD while avoiding double counting. It is worth noting that the results of LC-pCCD-λLDA and -λPBE are very similar to those from the global (MR+DFT) hybrid pCCD-λPBE in ref. 62. However, for the global hybrids the use of a GGA improves results upon LDA significantly,[62] while for range-separated hybrids LDA and PBE provide similar results. This can be rationalized by the fact that the LDA exchange and correlation terms are more accurate in the short range, as can be deduced from the exact SR expansions for these terms in eqn (18) and (19). In fact, LDA and PBE become equivalent at very large μ. Hence, the long-range correction has a more dramatic effect for LDA hybrids, because it takes out the part of the LDA which is most inaccurate and that is (to a certain extent) better described by semilocal approximations.

Apart from molecular dissociations, a common benchmark for MR+DFT methods is the Beryllium isoelectronic series (*i.e.*, $X^{(Z-4)+}$ ions). Be and its isoelectronic ions are difficult to describe by regular KS-DFT methods because of the static $s^2 \rightarrow p^2$ correlation which increases linearly with the nuclear charge Z. The double ionization potentials (IPs) given by various methods for this series are summarized in Table 2. These data are compared with accurate IPs calculated from total energies reported in ref. 95 and 96. For these calculations we use a Cartesian cc-pCVTZ(-f) basis, as we observed this basis set was accurate enough for our purpose: while total energies for the Helium isoelectronic $X^{(Z-2)+}$ ions go down by about 30 milihartrees when going from the cc-pVTZ(-f) basis to the cc-pCVTZ(-f) basis, the double IPs change no more than 1.7 milihartrees. In other words, the basis set incompleteness error due to the limited amount of core-polarization functions is canceled when taking energy differences between the $X^{(Z-2)+}$ and $X^{(Z-4)+}$ ions.

Because it misses dynamic correlation in the $X^{(Z-4)+}$ ions, pCCD tends to underestimate the IPs in Table 2 by, in average, 15.4 milihartree. Standard KS LDA has the largest mean absolute error (MAE) of all the methods in Table 2 (30.2 milihartree). It also has the largest nonparallelity error (NPE)—the difference between the maximum and minimum errors—as the quality of the LDA deteriorates badly with increasing charge. The pCCD-λLDA and LC-pCCD-LDA combinations do not really provide improvement upon pCCD; however, LC-pCCD-λLDA does improve upon its component methods (MAE = 3.9 milihartree). Compared to pCCD, LC-pCCD-PBE reduces the MAE but increases the NPE, whereas LC-pCCD-ωPBE has a similar MAE and a lower NPE; both methods are still much better than standard PBE. The best results are given by pCCD-λPBE (MAE = 2.8 milihartree) and LC-pCCD-$\lambda\omega$PBE (MAE = 1.7 milihartree). It is worth noting that LC-pCCD-$\lambda\omega$PBE yields results that are significantly better than LC-pCCD-λPBE, and that the latter does not improve upon its LDA variant. This can be explained by the fact that the LC-PBE exchange goes back to the LDA for large μ, whereas LC-ωPBE preserves the gradient corrections.[97] Nevertheless, like in the cases of bond breaking above, the inclusion of a fraction of short-range pCCD two-body energy appears to be important for obtaining good results. Also, we note again that the long-range correction with a fraction of SR pCCD two-body energy provides great improvement for LDA combinations, but not as much for PBE-based hybrids.

The results of ref. 62, and what we have seen here so far, indicate that pCCD-λPBE and LC-pCCD-λDFT (with LDA or PBE) can accurately describe the Be series as well as dissociations of single bonds. However, one of the difficulties for the previous pCCD-λDFT global hybrid is the description of the breaking of multiple bonds;[62] the method tends to overestimate binding energies of double and triple bonds. The reason for this is that pCCD goes to a too high energy limit at dissociation (higher than unrestricted Hartree–Fock). Hence, the range separation does not fix this issue. This is illustrated in Fig. 4, which shows the dissociation energy profiles for the double bond in formaldehyde and the triple bond of the nitrogen molecule. Only results by LDA-based combinations are shown in the Figure, but results with PBE combinations are very similar. Both LC-pCCD-DFT and -λDFT overestimate the the bond energies, although the overestimation by the latter is much smaller. A possible way to mitigate this overbinding is to use an unrestricted pCCD formalism (UpCCD). UpCCD methods are currently under investigation in our research group; preliminary tests suggest that they improve upon pCCD when the correlations are very strong and when pCCD displays largest errors, while having much less spin contamination than typical mean-field unrestricted approximations.

Table 2 Double ionization potentials for the Be isoelectronic series. The errors are in milihartrees; ME is the mean error, MAE the mean absolute error, and NPE the nonparallelity error. Hybrid pCCD+DFT calculations use λ = 0.75, μ = 0.4, and the [*n*,*m*] densities. The calculations use a Cartesian cc-pCVTZ(-f) basis. The accurate data are from ref. 95 and 96

		Errors (milihartrees)										
Ionization	Accurate IP (au)	pCCD	LDA	pCCD-λLDA	LC-pCCD-LDA	LC-pCCD-λLDA	PBE	pCCD-λPBE	LC-pCCD-PBE	LC-pCCD-ωPBE	LC-pCCD-λPBE	LC-pCCD-$\lambda\omega$PBE
$Be \rightarrow Be^{2+}$	1.0118	−7.9	23.4	17.2	11.4	4.3	−1.4	0.8	8.0	9.1	0.1	0.4
$B^{1+} \rightarrow B^{3+}$	2.3188	−12.0	11.2	15.3	12.6	5.3	−7.4	−1.2	8.8	13.5	−1.4	−0.2
$C^{2+} \rightarrow C^{4+}$	4.1289	−13.7	−2.1	14.3	8.0	5.3	−12.1	−1.5	6.4	16.5	−2.5	0.0
$N^{3+} \rightarrow N^{5+}$	6.4418	−15.7	−17.7	12.0	−1.7	3.3	−17.8	−2.5	1.0	16.8	−5.0	−1.0
$O^{4+} \rightarrow O^{6+}$	9.2560	−18.0	−34.8	9.0	−13.9	0.1	−23.9	−3.9	−5.2	16.3	−7.9	−2.5
$F^{5+} \rightarrow F^{7+}$	12.5703	−19.5	−52.2	6.4	−26.8	−2.9	−29.5	−4.6	−10.6	16.1	−10.0	−3.3
$Ne^{6+} \rightarrow Ne^{8+}$	16.3851	−20.8	−70.4	3.5	−40.5	−6.2	−35.4	−5.3	−15.6	15.9	−12.0	−4.2
ME		−15.4	−20.4	11.1	−7.3	1.3	−18.2	−2.6	−1.0	14.9	−5.5	−1.6
MAE		15.4	30.2	11.1	16.4	3.9	18.2	2.8	7.9	14.9	5.5	1.7
NPE		12.9	93.7	13.7	53.1	11.5	34.0	6.1	24.3	7.7	12.1	4.5

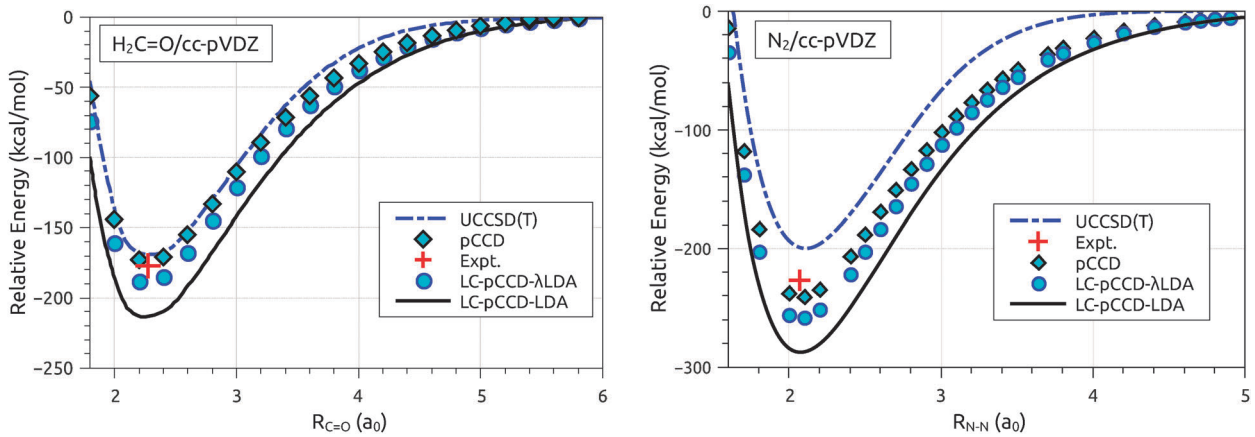

Fig. 4 Dissociation energy profiles for the CO bond in formaldehyde [r(HC) = 1.110 Å, HCO angle = 122.33°] and the nitrogen molecule. Hybrid methods use λ = 3/4 and μ = 0.4 au. All pCCD+DFT combinations use the [n,m] densities. Relative energies are with respect to the molecule at the dissociation limit. Cartesian basis sets are employed in all calculations.

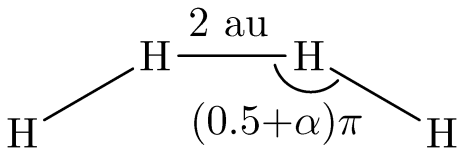

Fig. 5 The H_4 model system. All bond lengths are fixed at 2 au and the model a has mirror symmetry such that the parameter α uniquely determines the geometry.

As a last benchmark, we consider the H_4 model with the DZP basis of Paldus *et al.*[98–100] This model is shown schematically in Fig. 5; it consists of four hydrogen atoms in a trapezoidal configuration of C_{2v} symmetry; the nearest neighbor H–H distance is fixed at 2 au—this slight stretching enhances degeneracies—and therefore the geometry is uniquely determined by the $H_1H_2H_3$ bond angle, which is defined in terms of the parameter α as $\angle H_1H_2H_3 = (0.5 + \alpha)\pi$ radians. That is, the geometry is square at α = 0 and linear at α = 1/2. The DZP basis used consists of 5s primitves contracted to two basis functions with exponents (coefficients) of 33.6444 (0.025374), 5.05796 (0.1896829), 1.1468 (0.8529303) for the first function and 0.321144 (0.6068852), 0.101309 (0.4490200) for the second one, plus a polarization function with an exponent of 0.93.[98,100]

The total energies for the H_4/DZP model as a function of α predicted by pCCD and pCCD+PBE hybrids are compared with FCI data from ref. 99 in Fig. 6. LC-pCCD-$\lambda\omega$PBE and pCCD-λPBE are both similar and provide very good agreement with the FCI data from α = 0.01 to α = 0.5. In this region, pCCD recovers about 70–80% of the total correlation energy; at α = 0 pCCD captures only 46% of the total correlation and the quality of LC-pCCD-$\lambda\omega$PBE and pCCD-λPBE deteriorates too, although they still improve over pCCD. Interestingly though, methods incorporating lower amounts of pCCD two-body energy like LC-pCCD-ωPBE and pCCD-λPBE itself but with λ = 0.25, seem to yield too low energies in the α = 0.05–0.5 range, but improve the agreement with FCI at smaller values of α, including α = 0. This suggests that, as occurs for KS global and range separated hybrids,[87,89] the optimal amount of wavefunction energy is dependent on the system (even if only the geometry is varied, as in this case). Locally range-separated hybrids—where μ is itself a local functional of the density—have been suggested to overcome this defficiency of standard KS LC-DFT,[88,89] and this methodology can be extended to LC-pCCD+DFT without any

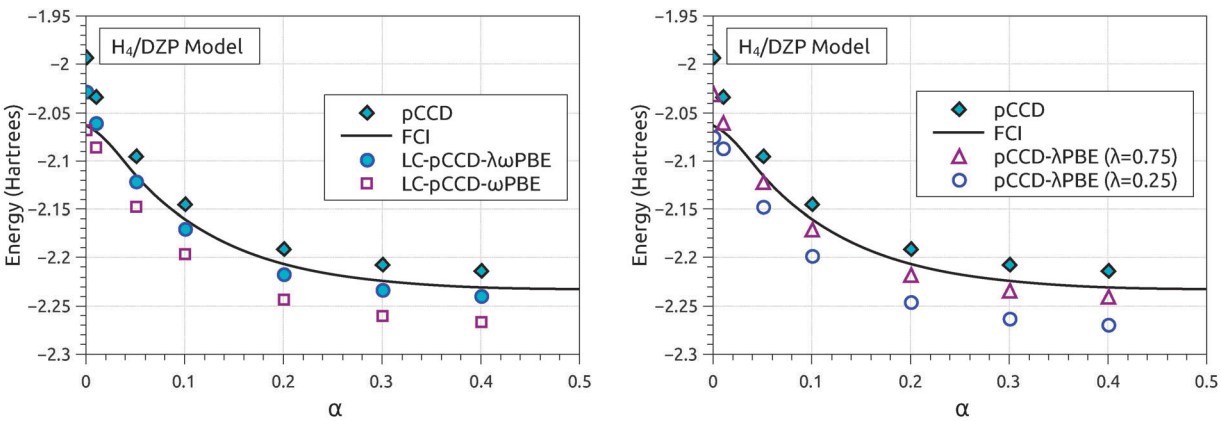

Fig. 6 Total energies for the H_4 model as a function of α with a DZP basis. Unless otherwise indicated, hybrid methods use λ = 0.75 and μ = 0.4 au.

formal difficulty. The practical disadvantage is that, as mentioned before, local range-separated hybrids are hard to implement and more expensive to evaluate than hybrids with fixed μ.[89] It is also likely that, just as in the case of dissociated N_2, employing the UpCCD formalism mentioned above will as well improve results at $\alpha = 0$ because restriced pCCD misses a large fraction of the correlation at this point and UpCCD would provide a better baseline for the addition of DFA dynamic correlation.

4 Concluding remarks

One can construct hybrids of pCCD and DFT (see Table 1) which are analogous to commonly used KS-DFT hybrids, except for a correction factor to E_c^{DFA} that accounts for double counting. These pCCD+DFT combinations can tackle the main problems of commonly used DFT approximations: the inclusion of substantial amounts of two-body wavefunction energy sharply decreases the SIE, whereas the use of a multireference wavefunction and the on-top pair density interpretation of KS-DFT address static correlation. The use of the alternative [*n*,*m*] densities is very important for the latter (even in range-separated hybrids), and this is the reason for which previous, similar, MR+DFT hybrids using MR densities directly provided unsatisfactory results for strongly correlated systems.[38] Among the range-separated schemes presented here, LC-pCCD-λLDA, -λPBE, and -$\lambda\omega$PBE are the most recommendable; the inclusion of a fraction of SR pCCD two-electron energy is important to obtain good results. Overall, the quality of these schemes is similar to that of our previous pCCD-λPBE global hybrid (although LC-pCCD-λLDA is substantially better that its global hybrid counterpart). It is also worth noting that it is straightforward to adapt the LC-pCCD+DFT methods presented here to create short-range hybrids analogous to, *e.g.*, the Heyd–Scuseria–Ernzerhof[101] (HSE) functional (*i.e.*, by just switching the ranges in eqn (14)). This opens the possibility to develop affordable short-range pCCD+DFT methods for describing static and dynamic correlations in solids. Likewise, extension to middle-range hybrids,[102] to achieve the accuracy of LR hybrids while preserving the computational advantages of SR hybrids, is also straightforward. Moreover, middle-range pCCD+DFT hybrids can be used to describe long-range weak interactions by using pCCD in the middle range and specialized van der Waals functionals[103–106] in the long-range.

Finally, we note that the formulas in Table 1 can be (and some have, indeed, already been) used to combine other MR methods with DFT. However, as we have noted before, pCCD has many features that make it more suitable for blending with DFT than traditional MR techniques of quantum chemistry: pCCD is black-box, has low scaling, is size-consistent and size-extensive, and its two-particle density matrix has only $2N^2$ nonzero elements. This last feature, the sparsity of the two-particle density matrix, allows for a computationally efficient use of the on-top pair density interpretation of KS-DFT, which we have seen here to be necessary to describe static correlation *via* MR+DFT (at least when commonly used density functional approximations are employed). We hope that all of this can stimulate the further development of pCCD+DFT methods.

Acknowledgements

This work was supported as part of the Center for the Computational Design of Functional Layered Materials, an Energy Frontier Research Center funded by the U.S. Department of Energy, Office of Science, Basic Energy Sciences under Award # DE-SC0012575. GES is a Welch Foundation chair (C-0036). We thank Andreas Savin for many helpful discussions and a critical reading of this manuscript.

References

1 A. J. Cohen, P. Mori-Sánchez and W. Yang, *Science*, 2008, **321**, 792.
2 J. P. Perdew and A. Zunger, *Phys. Rev. B: Condens. Matter Mater. Phys.*, 1981, **23**, 5048.
3 P. Mori-Sánchez, A. J. Cohen and W. Yang, *J. Chem. Phys.*, 2006, **125**, 201102.
4 A. Ruzsinszky, J. P. Perdew, G. I. Csonka, O. A. Vydrov and G. E. Scuseria, *J. Chem. Phys.*, 2006, **125**, 194112.
5 O. A. Vydrov, G. E. Scuseria and J. P. Perdew, *J. Chem. Phys.*, 2007, **126**, 154109.
6 J. P. Perdew, R. G. Parr, M. Levy and J. L. Balduz, *Phys. Rev. Lett.*, 1982, **49**, 1691.
7 B. Himmetoglu, A. Floris, S. de Gironcoli and M. Cococcioni, *Int. J. Quantum Chem.*, 2014, **114**, 14.
8 K. Capelle and V. L. Campo Jr., *Phys. Rep.*, 2013, **528**, 91.
9 A. Savin and H. Flad, *Int. J. Quantum Chem.*, 1995, **56**, 327.
10 H. Iikura, T. Tsuneda, T. Yanai and K. Hirao, *J. Chem. Phys.*, 2001, **115**, 3540.
11 T. Yanai, D. P. Tew and N. C. Handy, *Chem. Phys. Lett.*, 2004, **393**, 51.
12 O. A. Vydrov, J. Heyd, A. V. Krukau and G. E. Scuseria, *J. Chem. Phys.*, 2006, **125**, 074106.
13 O. A. Vydrov and G. E. Scuseria, *J. Chem. Phys.*, 2006, **125**, 234109.
14 D. Jacquemin, E. A. Perpète, O. A. Vydrov, G. E. Scuseria and C. Adamo, *J. Chem. Phys.*, 2007, **127**, 094102.
15 T. M. Henderson, A. F. Izmaylov, G. Scalmani and G. E. Scuseria, *J. Chem. Phys.*, 2009, **131**, 044108.
16 Y. Tawada, T. Tsuneda, S. Yanagisawa, T. Yanai and K. Hirao, *J. Chem. Phys.*, 2004, **120**, 8425.
17 M. Kamiya, H. Sekino, T. Tsuneda and K. Hirao, *J. Chem. Phys.*, 2005, **122**, 234111.
18 D. Jacquemin, E. A. Perpète, G. E. Scuseria, I. Ciofini and C. Adamo, *J. Chem. Theory Comput.*, 2008, **4**, 123.
19 E. A. Perpète, D. Jacquemin, C. Adamo and G. E. Scuseria, *Chem. Phys. Lett.*, 2008, **456**, 101.
20 D. Jacquemin, E. A. Perpète, M. Medved, G. Scalmani, M. J. Frisch, R. Kobayashi and C. Adamo, *J. Chem. Phys.*, 2007, **126**, 191108.
21 D. Jacquemin, E. A. Perpète, G. E. Scuseria, I. Ciofini and C. Adamo, *Chem. Phys. Lett.*, 2008, **465**, 226.
22 J. Song, M. A. Watson, H. Sekino and K. Hirao, *J. Chem. Phys.*, 2008, **129**, 024117.

23 T. Stein, L. Kronik and R. Baer, *J. Am. Chem. Soc.*, 2009, **131**, 2818.
24 L. Kronik, T. Stein, S. Refaely-Abramson and R. Baer, *J. Chem. Theory Comput.*, 2012, **8**, 1515.
25 R. Zaleśny, I. W. Bulik, W. Bartkowiak, J. M. Luis, A. Avramopoulos, M. G. Papadopoulos and P. Krawczyk, *J. Chem. Phys.*, 2010, **133**, 244308.
26 M. de Wergifosse and B. Champagne, *J. Chem. Phys.*, 2011, **134**, 074113.
27 A. J. Garza, G. E. Scuseria, S. B. Khan and A. M. Asiri, *Chem. Phys. Lett.*, 2013, **575**, 122.
28 J. Autschbach and M. Srebro, *Acc. Chem. Res.*, 2014, **47**, 2592.
29 A. J. Garza, N. A. Wazzan, A. M. Asiri and G. E. Scuseria, *J. Phys. Chem. A*, 2014, **118**, 11787.
30 G. C. Lie and E. Clementi, *J. Chem. Phys.*, 1974, **60**, 1275.
31 G. C. Lie and E. Clementi, *J. Chem. Phys.*, 1974, **60**, 1288.
32 R. Colle and O. Salvetti, *Theor. Chim. Acta*, 1979, **52**, 55.
33 F. Moscardó and E. San-Fabián, *Phys. Rev. A: At., Mol., Opt. Phys.*, 1991, **44**, 1549.
34 E. Kraka, *Chem. Phys.*, 1992, **161**, 149.
35 N. O. J. Malcolm and J. J. W. McDouall, *Phys. Rev.*, 1996, **100**, 10131.
36 N. O. J. Malcolm and J. J. W. McDouall, *J. Phys. Chem. A*, 1997, **101**, 8119.
37 T. Leininger, H. Stoll, H. Werner and A. Savin, *Chem. Phys. Lett.*, 1997, **275**, 151.
38 R. Pollet, A. Savin, T. Leininger and H. Stoll, *J. Chem. Phys.*, 2002, **116**, 1250.
39 W. Wu and S. Shaik, *Chem. Phys. Lett.*, 1999, **301**, 37.
40 S. Grimme and M. Waletzke, *J. Chem. Phys.*, 1999, **111**, 5645.
41 B. Miehlich, H. Stoll and A. Savin, *Mol. Phys.*, 1997, **91**, 527.
42 J. Gräfenstein and D. Cremer, *Chem. Phys. Lett.*, 2000, **316**, 569.
43 J. Gräfenstein and D. Cremer, *Mol. Phys.*, 2005, **103**, 279.
44 C. Gutlé and A. Savin, *Phys. Rev. A: At., Mol., Opt. Phys.*, 2007, **75**, 032519.
45 C. Gutlé, A. Savin, J. B. Krieger and J. Chen, *Int. J. Quantum Chem.*, 1999, **75**, 885.
46 H. Stoll, *Chem. Phys. Lett.*, 2003, **376**, 141.
47 R. Takeda, S. Yamanaka and K. Yamaguchi, *Chem. Phys. Lett.*, 2002, **366**, 321.
48 R. Takeda, S. Yamanaka and K. Yamaguchi, *Int. J. Quantum Chem.*, 2004, **96**, 463.
49 S. Gusarov, P. Malmqvist and R. Lindh, *Mol. Phys.*, 2004, **102**, 2207.
50 S. Gusarov, P. Malmqvist, R. Lindh and B. O. Roos, *Theor. Chem. Acc.*, 2004, **112**, 84.
51 A. J. Pérez-Jiménez and J. M. Pérez-Jordá, *Phys. Rev. A: At., Mol., Opt. Phys.*, 2007, **75**, 012503.
52 T. Tsuchimochi, G. E. Scuseria and A. Savin, *J. Chem. Phys.*, 2010, **132**, 024111.
53 K. Sharkas, A. Savin, H. J. A. Jensen and J. Tolouse, *J. Chem. Phys.*, 2012, **137**, 044104.
54 A. Stoyanova, A. M. Teale, J. Tolouse, T. Helgaker and E. Fromager, *J. Chem. Phys.*, 2013, **139**, 134113.
55 A. J. Garza, C. A. Jiménez-Hoyos and G. E. Scuseria, *J. Chem. Phys.*, 2013, **138**, 134102.
56 A. J. Garza, C. A. Jiménez-Hoyos and G. E. Scuseria, *J. Chem. Phys.*, 2014, **140**, 244102.
57 G. Li Manni, R. K. Carlson, S. Luo, D. Ma, J. Olsen, D. G. Truhlar and L. Gagliardi, *J. Chem. Theory Comput.*, 2014, **10**, 3669.
58 Y. Cornaton and E. Fromager, *Int. J. Quantum Chem.*, 2014, **114**, 1199.
59 J. D. Goodpaster, T. A. Barnes, F. R. Manby and T. F. Miller III, *J. Chem. Phys.*, 2014, **140**, 18A507.
60 E. Fromager, *Mol. Phys.*, 2015, **113**, 419.
61 E.D. Hedegård, S. Knecht, J.S. Kielberg, H.J. Aa.Jensen and M. Reiher, arXiv:1502.06157 [physics.chem-ph] (2015).
62 A. J. Garza, T. M. Henderson, I. W. Bulik and G. E. Scuseria, *J. Chem. Phys.*, 2015, **142**, 044109.
63 J. P. Perdew, A. Savin and K. Burke, *Phys. Rev. A: At., Mol., Opt. Phys.*, 1995, **51**, 4531.
64 K. Yamaguchi and T. Fueno, *Chem. Phys.*, 1977, **19**, 35.
65 A. D. Becke, A. Savin and H. Stoll, *Theor. Chim. Acta*, 1995, **91**, 147.
66 O. V. Gritsenko, R. R. T. Schipper and E. J. Baerends, *J. Chem. Phys.*, 1997, **107**, 5007.
67 G. Knizia and G. K. L. Chan, *Phys. Rev. Lett.*, 2012, **109**, 186404.
68 I. W. Bulik, G. E. Scuseria and J. Dukelsky, *Phys. Rev. B: Condens. Matter Mater. Phys.*, 2014, **89**, 035140.
69 C. A. Jiménez-Hoyos, T. M. Henderson, T. Tsuchimochi and G. E. Scuseria, *J. Chem. Phys.*, 2012, **136**, 164109.
70 S. R. White, *Phys. Rev. Lett.*, 1992, **69**, 2863.
71 P. A. Limacher, P. W. Ayers, P. A. Johnson, S. de Baerdemacker, D. van Neck and P. Bultinck, *J. Chem. Theory Comput.*, 2013, **9**, 1394.
72 P. A. Limacher, T. D. Kim, P. W. Ayers, P. A. Johnson, S. de Baerdemacker, D. van Neck and P. Bultinck, *Mol. Phys.*, 2014, **112**, 853.
73 P. Tecmer, K. Boguslawski, P. A. Johnson, P. A. Limacher, M. Chan, T. Verstraelen and P. W. Ayers, *J. Phys. Chem. A*, 2014, **118**, 9858.
74 K. Boguslawski, P. Tecmer, P. W. Ayers, P. Bultinck, S. de Baerdemacker and D. van Neck, *Phys. Rev. B: Condens. Matter Mater. Phys.*, 2014, **89**, 201106(R).
75 T. Stein, T. M. Henderson and G. E. Scuseria, *J. Chem. Phys.*, 2014, **140**, 214113.
76 T. M. Henderson, I. W. Bulik, T. Stein and G. E. Scuseria, *J. Chem. Phys.*, 2014, **141**, 244104.
77 L. Bytautas, T. M. Henderson, C. A. Jiménez-Hoyos, J. K. Ellis and G. E. Scuseria, *J. Chem. Phys.*, 2011, **135**, 044119.
78 M. J. Frisch, G. W. Trucks and H. B. Schegel, *et al.*, *Gaussian Development Version, Revision H.21*, Gaussian Inc., Wallingford, CT, 2009.
79 H. Stoll and A. Savin, *Density Functional Theory Methods in Physics*, eds. R. M. Dreizler and J. da Providencia, Plenum, New York, 1985, p. 177.
80 S. Paziani, S. Moroni, P. Gori-Giorgi and G. B. Bachelet, *Phys. Rev. B: Condens. Matter Mater. Phys.*, 2006, **73**, 155111.

81 E. Goll, H.-J. Werner and H. Stomm, *Phys. Chem. Chem. Phys.*, 2005, **7**, 3917.
82 J. Toulouse, F. Colonna and A. Savin, *J. Chem. Phys.*, 2005, **122**, 014110.
83 B. G. Janesko, T. M. Henderson and G. E. Scuseria, *J. Chem. Phys.*, 2009, **130**, 081105.
84 J. Toulouse, P. Gori-Giorgi and A. Savin, *Int. J. Quantum Chem.*, 2006, **106**, 2026.
85 E. Brémond and C. Adamo, *J. Chem. Phys.*, 2011, **135**, 024106.
86 E. Fromager, J. Tolouse and H. J. A. Jensen, *J. Chem. Phys.*, 2007, **126**, 074111.
87 S. Refaely-Abramson, R. Baer and L. Kronik, *Phys. Rev. B: Condens. Matter Mater. Phys.*, 2011, **84**, 075144.
88 A. V. Krukau, G. E. Scuseria, J. P. Perdew and A. Savin, *J. Chem. Phys.*, 2008, **129**, 124103.
89 T. M. Henderson, B. G. Janesko, G. E. Scuseria and A. Savin, *Int. J. Quantum Chem.*, 2009, **109**, 2023.
90 A. Karolewski, L. Kronik and S. Kümmel, *J. Chem. Phys.*, 2013, **138**, 204115.
91 J. P. Perdew, E. R. McMullen and A. Zunger, *Phys. Rev. A: At., Mol., Opt. Phys.*, 1981, **23**, 2785.
92 J. Toulouse, F. Colonna and A. Savin, *Phys. Rev. A: At., Mol., Opt. Phys.*, 2004, **70**, 062505.
93 P. M. W. Gill, R. D. Adamson and J. Pople, *Mol. Phys.*, 1996, **88**, 1005.
94 J. A. Pople, M. Head-Gordon and K. Raghavachari, *J. Chem. Phys.*, 1987, **87**, 5968.
95 A. J. Thakkar and T. Koga, *Phys. Rev. A: At., Mol., Opt. Phys.*, 1994, **50**, 854.
96 G. A. Petersson and S. L. Licht, *J. Chem. Phys.*, 1981, **75**, 4556.
97 T. M. Henderson, B. G. Janesko and G. E. Scuseria, *J. Chem. Phys.*, 2008, **128**, 194105.
98 X. Li and J. Paldus, *J. Chem. Phys.*, 1995, **103**, 1024.
99 P. Piecuch, R. Tobola and J. Paldus, *Int. J. Quantum Chem.*, 1995, **55**, 133.
100 J. Paldus, P. E. S. Wormer and M. Benard, *Collect. Czech. Chem. Commun.*, 1988, **53**, 1919.
101 J. Heyd, G. E. Scuseria and M. Ernzerhof, *J. Chem. Phys.*, 2003, **118**, 8207.
102 T. M. Henderson, A. F. Izmaylov, G. E. Scuseria and A. Savin, *J. Chem. Theory Comput.*, 2008, **4**, 1254.
103 M. Dion, H. Rydberg, E. Schröder, D. C. Langreth and B. I. Lundqvist, *Phys. Rev. Lett.*, 2004, **92**, 246401.
104 K. Lee, E. D. Murray, L. Kong, B. I. Lundqvist and D. C. Langreth, *Phys. Rev. B: Condens. Matter Mater. Phys.*, 2010, **82**, 081101(R).
105 O. A. Vydrov and T. Van Voorhis, *J. Chem. Phys.*, 2009, **130**, 104105.
106 T. Sato and H. Nakai, *J. Chem. Phys.*, 2009, **131**, 224104.

